
Analytical Characterization of the Accuracy of SLAM without Absolute Orientation Measurements

Anastasios I. Mourikis and Stergios I. Roumeliotis
{mourikis|stergios}@cs.umn.edu

*Dept. of Computer Science & Engineering
University of Minnesota
Minneapolis, MN 55455*

Multiple Autonomous
Robotic Systems (MARS) Lab

Technical Report
Number -2006-0001

August 2006

Dept. of Computer Science & Engineering
University of Minnesota
4-192 EE/CS Building
200 Union St. S.E.
Minneapolis, MN 55455
Tel: (612) 625-2217
Fax: (612) 625-0572
URL: <http://www.cs.umn.edu/~mourikis>

Analytical Characterization of the Accuracy of SLAM without Absolute Orientation Measurements

Anastasios I. Mourikis and Stergios I. Roumeliotis
{mourikis|stergios}@cs.umn.edu

Dept. of Computer Science & Engineering
University of Minnesota
Minneapolis, MN 55455

Multiple Autonomous Robotics Systems (MARS) Laboratory, TR-2006-0001

August 2006

Abstract

In this report we derive analytical upper bounds on the covariance of the state estimates in SLAM. The analysis is based on a novel formulation of the SLAM problem, that enables the simultaneous estimation of the landmark coordinates with respect to the a robot-centered frame (relative map), as well as with respect to a fixed global frame (absolute map). A study of the properties of the covariance matrix in this formulation yields *analytical* upper bounds for the uncertainty of both map representations. Moreover, by employing results from Least Squares estimation theory, the *guaranteed accuracy* of the robot pose estimates is derived as a function of the accuracy of the robot's sensors, and of the properties of the map. Contrary to previous approaches, the method presented here makes no assumptions about the availability of a sensor measuring the absolute orientation of the robot. The theoretical analysis is validated by simulation results and real-world experiments.

1 Introduction

Recent interest in Simultaneous Localization and Mapping (SLAM) has resulted in significant advances in the design of estimation algorithms [1, 2, 3, 4, 5], data association techniques [6], and sensor data processing [7, 8], that have enabled localization with maps consisting of millions of landmarks (e.g., [1]). However, a theoretical characterization of the attainable localization accuracy in SLAM remains an open problem to date. To the best of our knowledge, very few approaches exist in the literature, that focus on *predicting* the accuracy of the robot's pose and the map estimates, given the capabilities of a robot's sensor payload. As a result, evaluating the suitability of a robot with a given set of sensors for a particular application, largely remains a matter of exhaustive simulations and experimentation.

We here focus on deriving upper bounds for the covariance of the state estimates in SLAM, as a function of the accuracy of the robot's sensors and the size of the map. The derived closed-form expressions provide *theoretical guarantees* for the accuracy of SLAM, and can thus be employed during the design of a localization system, in order to determine the necessary accuracy of the robot's sensors. Contrary to previous approaches [9, 10], in the treatment presented here we need *not* assume that the robot is equipped with an absolute orientation sensor, and thus the problem formulation is more general. In order to derive analytical expressions for the upper bounds on the localization uncertainty, we employ a novel formulation of the SLAM problem, in which the landmark coordinates with respect to (i) the robot, and (ii) a fixed global frame, are jointly estimated. This enables us to derive upper bounds on the covariance of *both* map representations (cf. Section 3), as well as on the uncertainty in the robot's pose (cf. Section 5). Before delving into the details of our approach, in the following section we present an overview of related work.

2 Related Work

One of the first attempts to study the properties of the covariance matrix of the state estimates in SLAM was presented in [11]. In that work, a Linear Time Invariant (LTI) SLAM model is employed, in which both the robot and the landmarks are constrained to lie in a one-dimensional space. For this simple model, the solution to the Riccati differential equation, that describes the time evolution of the covariance matrix of the position estimates, is derived in closed form. This result demonstrates some of the properties of the covariance matrix in SLAM, but its practical importance is limited by the fact that the analysis holds only for motion in 1D, and for a LTI system model. The work of [11] has been extended to the case of a team of multiple vehicles performing SLAM [12] under the same set of restrictive assumptions (i.e., LTI system model, and motion in 1D).

A different set of properties of the covariance matrix in SLAM is studied in [13, 14, 15]. In particular, it is shown that the covariance matrix of the landmarks' position estimates is decreasing monotonically, as more observations are processed, and after sufficient time, the map estimates become fully correlated. Additionally, the authors derive a *lower bound* on the robot's and landmarks' covariance matrix, by considering the case in which the odometry measurements are *perfect*. Since no additional uncertainty is introduced in the system during state propagation, this is the "best-case scenario", and the covariance of the state estimates in this hypothetical system defines a lower bound, that depends only on the initial uncertainty of the robot's pose. These results are also extended to the case of *cooperative* Concurrent Mapping and Localization in [16, 17]. A limitation of the aforementioned approaches is that the derived lower bounds are *independent* of the accuracy of the robot's sensors, and thus cannot be employed in order to *compare* the performance of robots with sensors of different quality. Moreover, if the robot's initial pose is perfectly known, which is a common situation in SLAM, then these bounds are equal to zero, and are thus non-informative.

The work presented in this report is related to our previous work [9], in which upper bounds on the uncertainty of the position estimates in SLAM, as closed-form functions of the accuracy of the robot's sensors, are derived. In [9], it is assumed that the robot is equipped with an *absolute orientation* sensor (e.g., a compass). When such a sensor is available, the orientation uncertainty for the robot remains bounded, and the maximum variance of the orientation errors is known. This observation allows us to formulate a position-only Extended Kalman Filter estimator, and derive upper bounds for the asymptotic covariance of the state. This work is extended to the case of Cooperative SLAM in [10], under the assumption that every robot has an absolute orientation sensor. Clearly, such a requirement is constraining, and there exist cases where it is not satisfied. In this report, no absolute orientation measurements are assumed to be available, thus resulting in a more general formulation. As shown in Section 5, it is possible to derive an upper bound on the variance of the robot's orientation errors, *without* requiring that a compass or similar sensor be available.

3 The uncertainty of map estimation in SLAM

In this section, we derive upper bounds for the covariance of the landmarks' position estimates in SLAM. In particular, we derive upper bounds for the uncertainty of the landmarks' positions when these are expressed with respect to i) a fixed global frame (absolute map), and ii) the robot's coordinate frame (relative map).¹ Our approach is based on formulating an Extended Kalman Filter (EKF) estimator, in which the state vector is comprised of both the relative map coordinates, *and* the absolute map coordinates, but does *not* explicitly contain the robot pose. The estimate for the robot pose, as well as its covariance, can be inferred from the transformation between the two map representations, as shown in the following section.

Clearly, this formulation will not result in the most computationally efficient implementation of SLAM. However, the sole purpose of employing such a formulation of SLAM is to determine analytical upper bounds for the covariance of the state estimates. As will be made clear in the following, in the proposed EKF set-up *all* available measurements are used once, and apart from linearization, no other approximations are made. Therefore, the covariance of the absolute map computed with this filter will be identical (except for small linearization inaccuracies) to the covariance that is computed with the "traditional" EKF SLAM algorithm [18], in which the state vector contains the absolute map coordinates and the robot pose.

¹Note that the term "relative map" is used in this paper to describe a robot-centred map. This is different than the notion of the relative map employed, for example, in [13].

3.1 Relative-map SLAM

We first study the case in which the state vector is comprised only of the landmarks' positions with respect to the robot (relative map). Denoting the position of the i -th landmark with respect to the robot at time step ℓ by ${}^R p_{i_\ell}$, $i = 1 \dots N$, we obtain the following state propagation equation for this landmark:

$${}^R p_{i_{k+1}} = {}^{R_{k+1}} p_{R_k} + C(-\omega_k \delta t) {}^R p_{i_k} \quad (1)$$

where the rotation matrix expressing the rotation of the robot frame between time-steps $k+1$ and k is:

$$C(-\omega_k \delta t) = \begin{bmatrix} \cos(\omega_k \delta t) & \sin(\omega_k \delta t) \\ -\sin(\omega_k \delta t) & \cos(\omega_k \delta t) \end{bmatrix} \quad (2)$$

and ${}^{R_{k+1}} p_{R_k}$ is the position of the robot at time-step k , expressed with respect to the robot's frame at time-step $k+1$, which is given by:

$${}^{R_{k+1}} p_{R_k} = -C(-\omega_k \delta t) {}^{R_k} p_{R_{k+1}} = -v_k \delta t C(-\omega_k \delta t) e_1 \quad (3)$$

In the preceding expressions, v_k and ω_k are the translational and rotational velocity of the robot at time step k , respectively, δt is the sampling interval, and e_1 is the unit vector along the x -axis in the 2-dimensional space, i.e.,

$$e_1 = \begin{bmatrix} 1 \\ 0 \end{bmatrix}$$

Using the measurements of the robot's translational and rotational velocities, v_{m_k} and ω_{m_k} , respectively, the estimates for the landmarks' positions are propagated as follows:

$$\begin{aligned} {}^R \hat{p}_{i_{k+1}} &= {}^{R_{k+1}} \hat{p}_{R_k} + C(-\omega_{m_k} \delta t) {}^R \hat{p}_{i_k} \\ &= C(-\omega_{m_k} \delta t) (-v_{m_k} \delta t e_1 + {}^R \hat{p}_{i_k}) \end{aligned} \quad (4)$$

Clearly, the state propagation equation is nonlinear. By linearizing we obtain the error propagation equation for the relative position of the i -th landmark:

$${}^R \tilde{p}_{i_{k+1}} = C(-\omega_{m_k} \delta t) {}^R \tilde{p}_{i_k} - \delta t C(-\omega_{m_k} \delta t) e_1 \tilde{v}_k + \delta t J_{\times} {}^R \hat{p}_{i_k} \tilde{\omega}_k$$

In the last expression, the symbol \sim denotes the error in the estimate of the respective quantity, and

$$J_{\times} = \begin{bmatrix} 0 & 1 \\ -1 & 0 \end{bmatrix} \quad (5)$$

If we create a state vector, ${}^R \mathbf{X}$, that comprises of the relative positions of the landmarks with respect to the robot, then the error propagation equation for this state vector is:

$${}^R \tilde{\mathbf{X}}_{k+1} = {}^R \Phi_k {}^R \tilde{\mathbf{X}}_k + {}^R \mathbf{G}_k \begin{bmatrix} \tilde{v}_k \\ \tilde{\omega}_k \end{bmatrix} \quad (6)$$

where²

$${}^R \Phi_k = I_N \otimes C(-\omega_{m_k} \delta t) \quad (7)$$

and ${}^R \mathbf{G}_k$ is a $2N \times 2$ block matrix, whose i -th element is

$$G_{i_k} = \delta t \begin{bmatrix} -C(-\omega_{m_k} \delta t) e_1 & J_{\times} {}^R \hat{p}_{i_k} \end{bmatrix} \quad (8)$$

The covariance propagation equation for the uncertainty of the *relative map* is

$$\begin{aligned} {}^R \mathbf{P}_{k+1|k} &= {}^R \Phi_k {}^R \mathbf{P}_{k|k} {}^R \Phi_k^T + {}^R \mathbf{G}_k Q {}^R \mathbf{G}_k^T \\ &= {}^R \Phi_k {}^R \mathbf{P}_{k|k} {}^R \Phi_k^T + {}^R \mathbf{Q}_k \end{aligned} \quad (9)$$

²In the remainder of this report, I_n denotes the $n \times n$ identity matrix, $\mathbf{1}_{n \times m}$ denotes the $n \times m$ matrix of ones, $\mathbf{0}_{n \times m}$ denotes the $n \times m$ matrix of zeros, and \otimes denotes the Kronecker product.

where

$$Q = \text{diag}(\sigma_v^2, \sigma_\omega^2)$$

is the covariance matrix of the robot's odometric measurements, we have denoted

$${}^R\mathbf{Q}_k = {}^R\mathbf{G}_k Q {}^R\mathbf{G}_k^T,$$

and ${}^R\mathbf{P}_{k+1|k}$ and ${}^R\mathbf{P}_{k|k}$ are the covariance of the error in the state estimate of ${}^R\mathbf{X}(k+1)$ and ${}^R\mathbf{X}(k)$ respectively, after measurements up to time k have been processed.

3.2 The Dual-Map Filter

In order to introduce the absolute landmark coordinates in the state vector, we employ the following observation: without loss of generality, the global coordinate frame can be selected at the initial position of the robot. Thus, at the first time step, before the robot moves, the absolute map and the relative map *coincide*, i.e., ${}^G\mathbf{X} = {}^R\mathbf{X}_0$, where ${}^G\mathbf{X}$ is a vector that contains the coordinates of the N landmarks with respect to the fixed global frame. If at the first time step, we augment the state vector to include two identical copies of the state ${}^R\mathbf{X}_0$, and we thereafter propagate only one of the copies, while properly accounting for the correlations between the two, then at every time step an estimate for *both* the relative, and the absolute landmark coordinates will be available. This technique of state duplication is similar to the one employed in [19], with the difference that in our work the *landmark* states are duplicated, rather than the robot state.

The augmented state vector is equal to

$$\mathbf{X} = \begin{bmatrix} {}^R\mathbf{X} \\ {}^G\mathbf{X} \end{bmatrix}$$

and the error-state propagation equation is given by

$$\begin{aligned} \tilde{\mathbf{X}}_{k+1} &= \begin{bmatrix} {}^R\Phi_k & \mathbf{0}_{2N \times 2N} \\ \mathbf{0}_{2N \times 2N} & I_{2N} \end{bmatrix} \tilde{\mathbf{X}}_k + \begin{bmatrix} {}^R\mathbf{G}_k \\ \mathbf{0}_{2N \times 2} \end{bmatrix} \begin{bmatrix} \tilde{v}_k \\ \tilde{\omega}_k \end{bmatrix} \\ &= \Phi_k \tilde{\mathbf{X}}_k + \begin{bmatrix} I_{2N} \\ \mathbf{0}_{2N \times 2N} \end{bmatrix} {}^R\mathbf{G}_k \begin{bmatrix} \tilde{v}_k \\ \tilde{\omega}_k \end{bmatrix} \end{aligned} \quad (10)$$

while the covariance propagation equation is given by

$$\mathbf{P}_{k+1|k} = \Phi_k \mathbf{P}_{k|k} \Phi_k^T + \mathbf{G} {}^R\mathbf{Q}_k \mathbf{G}^T \quad (11)$$

with

$$\mathbf{G} = \begin{bmatrix} I_{2N} \\ \mathbf{0}_{2N \times 2N} \end{bmatrix}$$

Immediately after state duplication, and before the robot starts moving, the two copies of the state carry exactly the same information, and are thus fully correlated. As a result, the initial covariance matrix for the augmented state vector is given by:

$$\mathbf{P}_{0|0} = \begin{bmatrix} {}^R\mathbf{P}_{0|0} & {}^R\mathbf{P}_{0|0} \\ {}^R\mathbf{P}_{0|0} & {}^R\mathbf{P}_{0|0} \end{bmatrix} \quad (12)$$

At every time step, the robot measures the *relative position* of the landmarks, thus the measurement vector at each time step is described by

$$\mathbf{z}(k) = \begin{bmatrix} I_{2N} & \mathbf{0}_{2N \times 2N} \end{bmatrix} \mathbf{X}_k + \mathbf{n}(k) \quad (13)$$

where

$$\mathbf{H} = \begin{bmatrix} I_{2N} & \mathbf{0}_{2N \times 2N} \end{bmatrix}$$

is the measurement matrix, and $\mathbf{n}(k)$ is a Gaussian, zero-mean, white noise vector. Assuming that the errors in the measurement of each landmark are independent from the other robot-to-landmark measurement errors, then the covariance matrix of $\mathbf{n}(k)$ will be a generally time-varying, block-diagonal matrix:

$$\mathbf{R}_k = \text{Diag}(\mathbf{R}_{i_k}) \quad (14)$$

where R_{i_k} is the 2×2 covariance matrix of the measurement of the i -th landmark. Using these definitions, we can write the covariance update equation of the EKF as:

$$\mathbf{P}_{k+1|k+1} = \mathbf{P}_{k+1|k} - \mathbf{P}_{k+1|k} \mathbf{H}^T \mathbf{S}_{k+1}^{-1} \mathbf{H} \mathbf{P}_{k+1|k} \quad (15)$$

with

$$\mathbf{S}_{k+1} = \mathbf{H} \mathbf{P}_{k+1|k} \mathbf{H}^T + \mathbf{R}_k$$

At this point, a clarification regarding the structure of the measurement equation (cf. Eq. (13)) is due. At first, the fact that the measurement equation does not directly involve the absolute position estimates of the landmarks may appear somewhat peculiar. However, we remind that the correlations that exist between the relative and absolute position estimates of the landmarks guarantee that during the EKF update step, the absolute map estimates, as well as their covariance, are appropriately corrected. In other words, the close relation that exists between the absolute map and the relative map is expressed via the correlations in the augmented system covariance matrix.

By combining the covariance propagation and update equations (Eqs. (11) and (15)), we form the Riccati recursion that describes the time evolution of the covariance matrix in the augmented system. This is given by:

$$\mathbf{P}_{k+1} = \Phi_k (\mathbf{P}_k - \mathbf{P}_k \mathbf{H}^T \mathbf{S}_{k+1}^{-1} \mathbf{H} \mathbf{P}_k) \Phi_k^T + \mathbf{G}^R \mathbf{Q}_k \mathbf{G}^T \quad (16)$$

where we have introduced the substitutions $\mathbf{P}_k = \mathbf{P}_{k+1|k}$ and $\mathbf{P}_{k+1} = \mathbf{P}_{k+2|k+1}$ to simplify the notation.

In this work, we consider the case where the landmark positions are *unknown* prior to the first observation, and the robot has perfect initial knowledge of its pose, which is the most common setting for SLAM. Immediately after the first set of robot-to-landmark measurements, the uncertainty of the relative map is equal to the covariance matrix of these measurements, i.e., ${}^R\mathbf{P}_{0|0} = \mathbf{R}_0$. The initial value of the Riccati recursion is the covariance matrix for the dual-map filter, that arises after duplicating the initial state and performing one propagation step. Thus it is equal to:

$$\mathbf{P}_0 = \begin{bmatrix} \mathbf{R}_0 + {}^R\mathbf{Q}_0 & \mathbf{R}_0 \\ \mathbf{R}_0 & \mathbf{R}_0 \end{bmatrix} \quad (17)$$

4 Upper bounds on the Asymptotic Covariance

Having determined the Riccati recursion (Eq. (16)) and its initial value (Eq. (17)), we are now able to derive an upper bound for its solution, and thus an upper bound on the covariance of the map in SLAM, by a method similar to that of [10]. For this purpose, we employ the following lemma:

Lemma 4.1 *If \mathbf{R}_u and \mathbf{Q}_u are constant matrices such that $\mathbf{R}_u \succeq \mathbf{R}_k$ and $\mathbf{Q}_u \succeq {}^R\mathbf{Q}_k$, for all $k \geq 1$, then the solution to the Riccati recursion*

$$\mathbf{P}_{k+1}^u = \Phi_k (\mathbf{P}_k^u - \mathbf{P}_k^u \mathbf{H}^T (\mathbf{H} \mathbf{P}_k^u \mathbf{H}^T + \mathbf{R}_u)^{-1} \mathbf{H} \mathbf{P}_k^u) \Phi_k^T + \mathbf{G} \mathbf{Q}_u \mathbf{G}^T \quad (18)$$

with an initial condition \mathbf{P}_0^u such that $\mathbf{P}_0^u \succeq \mathbf{P}_0$, satisfies $\mathbf{P}_k^u \succeq \mathbf{P}_k$ for all $k \geq 0$.

Proof: See Appendix A.

We now show how upper bounds on the matrices ${}^R\mathbf{Q}_k$, \mathbf{R}_k , and \mathbf{P}_0 can be obtained. We start by rewriting the system noise covariance matrix ${}^R\mathbf{Q}_k$, as (cf. Eqs. (8) and (10)):

$${}^R\mathbf{Q}_k = \underbrace{\delta t^2 \sigma_v^2 \cdot {}^R\Phi_k \mathbf{v} \mathbf{v}^T ({}^R\Phi_k)^T}_{\mathbf{Q}_{v_k}} + \underbrace{\delta t^2 \sigma_\omega^2 \cdot (I_N \otimes J_\times) {}^R\mathbf{X}_k {}^R\mathbf{X}_k^T (I_N \otimes J_\times)^T}_{\mathbf{Q}_{\omega_k}} \quad (19)$$

where

$$\mathbf{v} = \begin{bmatrix} 1 \\ 0 \\ 1 \\ 0 \\ \vdots \end{bmatrix} = \mathbf{1}_{N \times 1} \otimes e_1$$

We now consider each of the components of ${}^R\mathbf{Q}_k$ independently. For \mathbf{Q}_{v_k} we obtain:

$$\mathbf{Q}_{v_k} = \delta t^2 \sigma_v^2 \cdot {}^R\Phi_k \mathbf{v} \mathbf{v}^T ({}^R\Phi_k)^T \quad (20)$$

$$\preceq \delta t^2 \sigma_v^2 \cdot {}^R\Phi_k (\mathbf{v} \mathbf{v}^T + \mathbf{u} \mathbf{u}^T) ({}^R\Phi_k)^T \quad (21)$$

where

$$\mathbf{u} = \begin{bmatrix} 0 \\ 1 \\ 0 \\ 1 \\ \vdots \end{bmatrix} = \mathbf{1}_{N \times 1} \otimes e_2$$

We now note that

$$\mathbf{v} \mathbf{v}^T + \mathbf{u} \mathbf{u}^T = \mathbf{1}_{N \times N} \otimes I_2 \quad (22)$$

and thus

$$\mathbf{Q}_{v_k} \preceq \delta t^2 \sigma_v^2 \cdot {}^R\Phi_k (\mathbf{1}_{N \times N} \otimes I_2) ({}^R\Phi_k)^T \quad (23)$$

$$= \delta t^2 \sigma_v^2 (\mathbf{1}_{N \times N} \otimes I_2) \quad (24)$$

For the term \mathbf{Q}_{ω_k} we obtain:

$$\text{trace}(\mathbf{Q}_{\omega_k}) = \delta t^2 \sigma_\omega^2 \text{trace}((I_N \otimes J_\times)^R \mathbf{X}_k {}^R\mathbf{X}_k^T (I_N \otimes J_\times)^T) \quad (25)$$

$$= \delta t^2 \sigma_\omega^2 \text{trace}({}^R\mathbf{X}_k^T (I_N \otimes J_\times)^T (I_N \otimes J_\times)^R \mathbf{X}_k) \quad (26)$$

$$= \delta t^2 \sigma_\omega^2 \text{trace}({}^R\mathbf{X}_k^T {}^R\mathbf{X}_k) \quad (27)$$

$$= \sigma_\omega^2 \delta t^2 \sum_{i=1}^N \rho_i^2 \quad (28)$$

where ρ_i is the distance of the i -th landmark to the robot. Thus, if ρ_o is the maximum possible distance between the robot and any landmark (determined, for example, by the robot's maximum sensing range), we obtain

$$\text{trace}(\mathbf{Q}_{\omega_k}) \leq N \rho_o^2 \sigma_\omega^2 \delta t^2$$

and therefore

$$\mathbf{Q}_{\omega_k} \preceq N \rho_o^2 \sigma_\omega^2 \delta t^2 I_{2N} \quad (29)$$

By combining this result with those of Eqs. (19) and (24), we obtain:

$${}^R\mathbf{Q}_k \preceq \delta t^2 \sigma_v^2 (\mathbf{1}_{N \times N} \otimes I_2) + N \rho_o^2 \sigma_\omega^2 \delta t^2 I_{2N} = q_1 (\mathbf{1}_{N \times N} \otimes I_2) + q_2 I_{2N} \quad (30)$$

And thus an upper bound for ${}^R\mathbf{Q}_k$ is given by the matrix

$$\mathbf{Q}_u = \underbrace{\delta t^2 \sigma_v^2 (\mathbf{1}_{N \times N} \otimes I_2)}_{q_1} + \underbrace{N \rho_o^2 \sigma_\omega^2 \delta t^2 I_{2N}}_{q_2} \quad (31)$$

$$= q_1 (\mathbf{1}_{N \times N} \otimes I_2) + q_2 I_{2N} \quad (32)$$

An upper bound on the measurement covariance matrix, \mathbf{R}_k , can be derived by considering the characteristics of the particular sensor used for the relative position measurements. If the covariance matrix of the measurement of each individual landmark can be bounded above by $R_{i_k} \preceq r I_2$, then we obtain

$$\mathbf{R}_k \preceq r I_{2N} = \mathbf{R}_u$$

Regarding the initial value of the recursion in Eq. (18), it is easy to see that the following matrix satisfies the condition $\mathbf{P}_0^u \succeq \mathbf{P}_0$:

$$\mathbf{P}_0^u = \begin{bmatrix} \mathbf{Q}_u + r I_{2N} & r I_{2N} \\ r I_{2N} & r I_{2N} \end{bmatrix} \quad (33)$$

An additional difficulty in solving for the steady-state value of the Riccati recursion in Eq. (18) is that the state transition matrix, Φ_k , is time-varying. Considering however the special structure of the matrices that appear in this recursion, the following lemma can be proven:

Lemma 4.2 Let the solution, \mathbf{P}_k^u , to the recursion in Eq. (18) be partitioned in $2N \times 2N$ blocks as

$$\mathbf{P}_k^u = \begin{bmatrix} {}^R\mathbf{P}_k^u & \mathbf{P}_{RG_k} \\ \mathbf{P}_{RG_k}^T & {}^G\mathbf{P}_k^u \end{bmatrix} \quad (34)$$

Additionally, let $\bar{\mathbf{P}}_k$ be the solution to the recursion

$$\bar{\mathbf{P}}_{k+1} = \bar{\mathbf{P}}_k - \bar{\mathbf{P}}_k \mathbf{H}^T (\mathbf{H} \bar{\mathbf{P}}_k \mathbf{H}^T + \mathbf{R}_u)^{-1} \mathbf{H} \bar{\mathbf{P}}_k + \mathbf{G} \mathbf{Q}_u \mathbf{G}^T \quad (35)$$

with initial condition $\bar{\mathbf{P}}_0 = \mathbf{P}_0^u$, and let $\bar{\mathbf{P}}_k$ be partitioned as

$$\bar{\mathbf{P}}_k = \begin{bmatrix} {}^R\bar{\mathbf{P}}_k & \bar{\mathbf{P}}_{RG_k} \\ \bar{\mathbf{P}}_{RG_k}^T & {}^G\bar{\mathbf{P}}_k \end{bmatrix} \quad (36)$$

Then for any $k \geq 0$, and for the transition matrix Φ_k defined in Eq. (10), the following relations hold:

$${}^R\bar{\mathbf{P}}_k = {}^R\mathbf{P}_k^u, \quad {}^G\bar{\mathbf{P}}_k = {}^G\mathbf{P}_k^u, \quad \text{and} \quad \mathbf{P}_{RG_k} = {}^R\mathbf{C}_k \bar{\mathbf{P}}_{RG_k} \quad (37)$$

where ${}^R\mathbf{C}_k = {}^R\Phi_k \cdot {}^R\Phi_{k-1} \cdots {}^R\Phi_0$.

Proof: See Appendix B

This lemma essentially demonstrates, that in order to derive the upper bound on the steady-state covariance of both the absolute and the relative map in SLAM, it suffices to determine the steady-state solution of the Riccati in Eq. (35), which is significantly simpler than that of Eq. (18), since it is a *constant coefficient* Riccati recursion. In order to determine the *asymptotic* solution of Eq. (35), we employ the following lemma, which has been adapted from [20]:

Lemma 4.3 Suppose $\bar{\mathbf{P}}_k^{(0)}$ is the solution to the discrete time Riccati recursion in Eq. (35) with initial value $\bar{\mathbf{P}}_0^u = \mathbf{0}_{4N \times 4N}$. Then the solution with the initial condition given in Eq. (33) is determined by the identity

$$\bar{\mathbf{P}}_k^u - \bar{\mathbf{P}}_k^{(0)} = \mathbf{T}_k (I_{4N} + \bar{\mathbf{P}}_0 \mathbf{J}_k)^{-1} \bar{\mathbf{P}}_0 \mathbf{T}_k^T \quad (38)$$

where \mathbf{T}_k is given by

$$\mathbf{T}_k = (I_{4N} - \mathbf{K}_p \mathbf{H})^k (I_{4N} + \mathbf{P} \mathbf{J}_k) \quad (39)$$

In these expressions, \mathbf{P} is any solution to the Discrete Algebraic Riccati Equation (DARE):

$$\mathbf{P} = \mathbf{P} - \mathbf{P} \mathbf{H}^T (\mathbf{H} \mathbf{P} \mathbf{H}^T + \mathbf{R}_u)^{-1} \mathbf{H} \mathbf{P} + \mathbf{G} \mathbf{Q}_u \mathbf{G}^T \quad (40)$$

and $\mathbf{K}_p = \mathbf{P} \mathbf{H}^T (\mathbf{R}_u + \mathbf{H} \mathbf{P} \mathbf{H}^T)^{-1}$. \mathbf{J}_k denotes the solution to the dual Riccati recursion:

$$\mathbf{J}_{k+1} = \mathbf{J}_k - \mathbf{J}_k \mathbf{G} (\mathbf{Q}_u^{-1} + \mathbf{G}^T \mathbf{J}_k \mathbf{G})^{-1} \mathbf{G}^T \mathbf{J}_k + \mathbf{H}^T \mathbf{R}_u^{-1} \mathbf{H} \quad (41)$$

with zero initial condition, $\mathbf{J}_0 = 0$.

Lemma 4.3 simplifies the evaluation of the steady-state value of $\bar{\mathbf{P}}_k$, since the solution to the Riccati recursion with zero initial condition is easily derived. This is because when the initial value of the covariance is zero, then the submatrix of $\bar{\mathbf{P}}_k$ that corresponds to the covariance of the absolute map will *remain* zero for all $k \geq 0$, since no influx of uncertainty occurs in the absolute landmark coordinates. This observation results in significant simplification of the derivations necessary to obtain the solution.

Applying Lemmas 4.3 and 4.2, and evaluating the limit of the resulting expressions as $k \rightarrow \infty$, allows us to obtain the following upper bound for the asymptotic covariance matrix of the augmented-state filter (cf. Appendix C):

$$\mathbf{P}_\infty \preceq \begin{bmatrix} \mathbf{U} \text{diag} \left(\frac{\lambda_i}{2} + \sqrt{\frac{\lambda_i^2}{4} + \lambda_i r} \right) \mathbf{U}^T & \mathbf{0}_{2N \times 2N} \\ \mathbf{0}_{2N \times 2N} & \mathbf{U} \text{diag} \left(-\frac{\lambda_i}{2} + \sqrt{\frac{\lambda_i^2}{4} + \lambda_i r} \right) \mathbf{U}^T \end{bmatrix} \quad (42)$$

where we have denoted the eigenvalue decomposition of \mathbf{Q}_u as $\mathbf{Q}_u = \mathbf{U} \text{diag}(\lambda_i) \mathbf{U}^T$. This expression provides an upper bound for the covariance of the augmented state vector after every EKF *propagation* step. In order to derive a bound for the covariance immediately after the *update* step of the EKF, we note that during propagation, the absolute map covariance remains unchanged, while the uncertainty of the relative map is increased according to Eq. (9). Using this observation, we can show that an upper bound on the steady-state covariance matrix of the relative map, immediately after every update step, is given by

$${}^R\bar{\mathbf{P}}_\infty = \mathbf{U} \text{diag} \left(-\frac{\lambda_i}{2} + \sqrt{\frac{\lambda_i^2}{4} + \lambda_i r} \right) \mathbf{U}^T \quad (43)$$

while the asymptotic uncertainty of the absolute positions of the landmarks in SLAM is bounded above by the matrix

$${}^G\bar{\mathbf{P}}_\infty = \mathbf{U} \text{diag} \left(-\frac{\lambda_i}{2} + \sqrt{\frac{\lambda_i^2}{4} + \lambda_i r} \right) \mathbf{U}^T \quad (44)$$

It is interesting to note that the special structure of the matrix \mathbf{Q}_u (cf. Eq. (32)) allows us to compute its eigenvalues in closed form. Specifically, it can be shown that \mathbf{Q}_u has 2 singular values equal to $\lambda_i = Nq_1 + q_2$, and $2N - 2$ singular values equal to $\lambda_i = q_2$. As a result, the above upper bounds will have two singular values equal to

$$\lambda_{p_i} = -\frac{Nq_1 + q_2}{2} + \sqrt{\frac{(Nq_1 + q_2)^2}{4} + (Nq_1 + q_2)r}, \quad i = 1, 2 \quad (45)$$

and $2N - 2$ eigenvalues equal to

$$\lambda_{p_i} = -\frac{q_2}{2} + \sqrt{\frac{q_2^2}{4} + q_2 r}, \quad i = 3, \dots, 2N \quad (46)$$

Moreover, the upper bounds will have a structure similar to the that of \mathbf{Q}_u , i.e.,

$${}^R\bar{\mathbf{P}}_\infty = {}^G\bar{\mathbf{P}}_\infty = b_1(\mathbf{1}_{N \times N} \otimes I_2) + b_2 I_{2N} \quad (47)$$

where

$$b_1 = -\frac{q_1}{2} + \frac{1}{N} \sqrt{\frac{(Nq_1 + q_2)^2}{4} + (Nq_1 + q_2)r} - \frac{1}{N} \sqrt{\frac{q_2^2}{4} + q_2 r} \quad (48)$$

and

$$b_2 = -\frac{q_2}{2} + \sqrt{\frac{q_2^2}{4} + q_2 r} \quad (49)$$

We note that the the result of Eq. (47) provides bounds for the accuracy of the map in SLAM, that are evaluated in closed form, and depend on the accuracy of the robot's sensors, as well on the size of the area being mapped. Interestingly, the *bounds* on the both the relative and the absolute map are *equal*, when the covariance matrix after the update phase of the EKF is considered. However, it should be clear that the *actual* covariance matrices of the two map representations are *not* identical at steady state. In the next section, we show how these results can be employed in order to obtain bounds on the covariance of the robot's pose estimates in SLAM.

5 The accuracy of pose estimation in SLAM

Although the robot pose (position and orientation) is not explicitly contained in the state vector of the formulation that we presented in the preceding section, an estimate for this pose is implicitly defined from the estimates of the relative map, ${}^R\mathbf{X}$, and of the absolute map, ${}^G\mathbf{X}$. To see why this is the case, we note that for the i -th landmark, the relation between its representation in the global frame, ${}^G p_i$, and in the robot frame at time step k , ${}^{R_k} p_i$, is given by:

$${}^G p_i = {}^G p_{R_k} + C(\phi_k) {}^{R_k} p_i \quad (50)$$

where ${}^G p_{R_k}$ and ϕ_k are the position and orientation of the robot with respect to the global frame at time step k , respectively. Thus, given the augmented state vector at time-step k , $\mathbf{X}_k = [{}^R \mathbf{X}^T \quad {}^G \mathbf{X}^T]^T$, and its covariance, \mathbf{P}_k , we are able to determine the robot pose,

$$\boldsymbol{\theta}_k = [{}^G p_{R_k}^T \quad \phi_k]^T$$

and its covariance, $\mathbf{P}_{\boldsymbol{\theta}\boldsymbol{\theta}}$, by solving the Least Squares minimization problem:

$$\min_{\boldsymbol{\theta}_k} \mathbf{e}_k^T \mathbf{W}_k^{-1} \mathbf{e}_k \quad (51)$$

where \mathbf{e}_k is the vector of errors that we seek to minimize, a $2N \times 1$ vector, whose i -th block is equal to

$$e_i = {}^G p_{R_k} + C(\phi_k)^{R_k} p_i - {}^G p_i \quad (52)$$

and \mathbf{W}_k is the covariance matrix of the vector \mathbf{e}_k . Employing linearization of Eq. (52), we obtain

$$\mathbf{W}_k = \mathbf{H}_{X_k} \mathbf{P}_k \mathbf{H}_{X_k}^T \quad (53)$$

where \mathbf{H}_{X_k} is the Jacobian of the error vector \mathbf{e}_k with respect to the state vector \mathbf{X}_k , given by

$$\mathbf{H}_{X_k} = [I_{2N} \otimes C(\phi_k) \quad I_{2N}] \quad (54)$$

It is known from the theory of Least Squares Estimation that the covariance matrix of the estimated parameter, $\boldsymbol{\theta}_k$, is given by

$$\begin{aligned} \mathbf{P}_{\boldsymbol{\theta}\boldsymbol{\theta}} &= (\mathbf{H}_{\boldsymbol{\theta}_k}^T \mathbf{W}_k^{-1} \mathbf{H}_{\boldsymbol{\theta}_k})^{-1} \\ &= \left(\mathbf{H}_{\boldsymbol{\theta}_k}^T (\mathbf{H}_{X_k} \mathbf{P}_k \mathbf{H}_{X_k}^T)^{-1} \mathbf{H}_{\boldsymbol{\theta}_k} \right)^{-1} \end{aligned} \quad (55)$$

where $\mathbf{H}_{\boldsymbol{\theta}_k}$ is the Jacobian matrix of the error vector \mathbf{e}_k with respect to $\boldsymbol{\theta}_k$. This is a $2N \times 3$ block matrix, whose i -th block element is equal to

$$H_i = [I_2 \quad \check{p}_{i_k}] \quad (56)$$

where we have denoted $\check{p}_{i_k} = -J_{\times} C(\phi_k)^{R_k} p_i$. We point out that the solution of the Least Squares problem in Eq. (51) and the covariance of this solution, given by Eq. (55), yield the *same* results for the robot's pose, as the "standard" EKF formulation for SLAM, when at least 2 landmarks are available. This is because in both cases, *all* the available measurements are used, and no approximations are made (apart from linearization). Thus, we can use the expression of Eq. (55), to study the properties of the robot pose covariance in EKF-based SLAM.

In the following, we focus on deriving upper bounds on the steady-state value of the matrix $\mathbf{P}_{\boldsymbol{\theta}\boldsymbol{\theta}}$. Note that since $\mathbf{P}_k \preceq \mathbf{P}_k^u$, an upper bound for the covariance of the robot pose at time-step k is given by (cf. Eq. (55)):

$$\mathbf{P}_{\boldsymbol{\theta}\boldsymbol{\theta}}^u = \left(\mathbf{H}_{\boldsymbol{\theta}_k}^T (\mathbf{H}_{X_k} \mathbf{P}_k^u \mathbf{H}_{X_k}^T)^{-1} \mathbf{H}_{\boldsymbol{\theta}_k} \right)^{-1} \quad (57)$$

Using the asymptotic results from Eq. (47) and the values of the Jacobian \mathbf{H}_{X_k} from Eq. (54), we obtain:

$$\mathbf{H}_{X_k} \mathbf{P}_{\infty}^u \mathbf{H}_{X_k}^T = 2b_1(\mathbf{1}_{N \times N} \otimes I_2) + 2b_2 I_{2N} \Rightarrow \quad (58)$$

$$\left(\mathbf{H}_{X_k} \mathbf{P}_{\infty}^u \mathbf{H}_{X_k}^T \right)^{-1} = \underbrace{\frac{1}{2b_2}}_{\alpha} I_{2N} - \underbrace{\frac{b_1}{b_2(2b_2 + 2b_1 N)}}_{\beta} (\mathbf{1}_{N \times N} \otimes I_2) \quad (59)$$

$$= \alpha I_{2N} - \beta (\mathbf{1}_{N \times N} \otimes I_2) \quad (60)$$

where we have used the result of Appendix D. Substitution in Eq. (57) yields the following asymptotic value for $\mathbf{P}_{\boldsymbol{\theta}\boldsymbol{\theta}}^u$:

$$\mathbf{P}_{\boldsymbol{\theta}\boldsymbol{\theta}}^u = \begin{bmatrix} (\alpha N - \beta N^2) I_2 & (\alpha - \beta N) \sum_{i=1}^N \check{p}_i \\ (\alpha - \beta N) \sum_{i=1}^N \check{p}_i^T & \alpha \sum_{i=1}^N (\check{p}_i^T \check{p}_i) - \beta \left(\sum_{i=1}^N \check{p}_i \right)^T \left(\sum_{i=1}^N \check{p}_i \right) \end{bmatrix}^{-1} = \begin{bmatrix} P_{PP} & P_{P\phi} \\ P_{P\phi}^T & P_{\phi\phi} \end{bmatrix} \quad (61)$$

Employing the formula for the inversion of a partitioned matrix (cf. Appendix E), we obtain the following expression for $P_{\phi\phi}$, which is an upper bound of the asymptotic orientation variance:

$$P_{\phi\phi} = \frac{1}{\alpha} \frac{1}{\sum_{i=1}^N (\check{p}_i^T \check{p}_i) - \frac{1}{N} \left(\sum_{i=1}^N \check{p}_i^T \right) \left(\sum_{i=1}^N \check{p}_i \right)} \quad (62)$$

For any i, j , the property $\check{p}_i^T \check{p}_j = {}^R p_i^T {}^R p_j$ holds, and thus we can re-write the denominator of the expression for $P_{\phi\phi}$ as

$$D = \frac{1}{N} \left(N \sum_{i=1}^N ({}^R p_i^T {}^R p_i) - \left(\sum_{i=1}^N {}^R p_i^T \right) \left(\sum_{i=1}^N {}^R p_i \right) \right)$$

Moreover, if we denote the distance between landmarks i and j as ρ_{ij} , we obtain

$$\begin{aligned} \sum_{i=1}^N \sum_{j=1}^N \rho_{ij}^2 &= \sum_{i=1}^N \sum_{j=1}^N ({}^R p_i - {}^R p_j)^T ({}^R p_i - {}^R p_j) \\ &= \sum_{i=1}^N \left(\sum_{j=1}^N ({}^R p_i^T {}^R p_i) + \sum_{j=1}^N ({}^R p_j^T {}^R p_j) - 2 \sum_{j=1}^N ({}^R p_j^T {}^R p_i) \right) \\ &= \sum_{i=1}^N \left(N {}^R p_i^T {}^R p_i + \sum_{j=1}^N ({}^R p_j^T {}^R p_j) - 2 {}^R p_i^T \left(\sum_{j=1}^N {}^R p_j \right) \right) \\ &= N \sum_{i=1}^N ({}^R p_i^T {}^R p_i) + N \sum_{j=1}^N ({}^R p_j^T {}^R p_j) - 2 \left(\sum_{i=1}^N {}^R p_i^T \right) \left(\sum_{j=1}^N {}^R p_j \right) \\ &= 2 \left(N \sum_{i=1}^N ({}^R p_i^T {}^R p_i) - \left(\sum_{i=1}^N {}^R p_i^T \right) \left(\sum_{i=1}^N {}^R p_i \right) \right) \\ &= 2ND \end{aligned} \quad (63)$$

Using this result, the upper bound on the robot's orientation uncertainty is written as:

$$P_{\phi\phi} = \frac{1}{\alpha} \frac{2N}{\sum_{i=1}^N \sum_{j=1}^N \rho_{ij}^2} = \frac{4Nb_2}{\sum_{i=1}^N \sum_{j=1}^N \rho_{ij}^2} \quad (64)$$

Thus, if the pairwise distances of the landmarks are known, an upper bound on the robots' orientation variance is determined by the preceding expression. Furthermore, if some properties of the placement of the landmarks in space is known, this expression can be employed in order to determine bounds that are independent of the *actual* landmark positions. For example, if the minimum allowable distance between any two landmarks is equal to $\rho_{LL\min}^2$, then

$$P_{\phi\phi} \leq \frac{1}{\alpha} \frac{2}{(N-1)\rho_{LL\min}^2} = \frac{4b_2}{(N-1)\rho_{LL\min}^2} \quad (65)$$

We now show how an upper bound on the covariance matrix of the robot's position estimates can be determined. From Eq. (61) we obtain:

$$P_{PP} = \left((\alpha N - \beta N^2) I_2 - \frac{(\alpha - \beta N)^2}{\alpha \sum_{i=1}^N (\check{p}_i^T \check{p}_i) - \beta \left(\sum_{i=1}^N \check{p}_i^T \right) \left(\sum_{i=1}^N \check{p}_i \right)} \left(\sum_{i=1}^N \check{p}_i \right) \left(\sum_{i=1}^N \check{p}_i^T \right) \right)^{-1}$$

which, by application of the matrix inversion lemma (cf. Appendix D) and simple manipulation, yields:

$$P_{PP} = \frac{1}{\alpha N - \beta N^2} I_2 + \frac{\left(\sum_{i=1}^N \check{p}_i \right) \left(\sum_{i=1}^N \check{p}_i^T \right)}{\alpha N^2 \left(\sum_{i=1}^N (\check{p}_i^T \check{p}_i) - \frac{1}{N} \left(\sum_{i=1}^N \check{p}_i^T \right) \left(\sum_{i=1}^N \check{p}_i \right) \right)}$$

$$= \frac{2b_2 + 2Nb_1}{N} I_2 + \underbrace{\frac{2b_2 \left(\sum_{i=1}^N \check{p}_i \right) \left(\sum_{i=1}^N \check{p}_i^T \right)}{N^2 \left(\sum_{i=1}^N (\check{p}_i^T \check{p}_i) - \frac{1}{N} \left(\sum_{i=1}^N \check{p}_i^T \right) \left(\sum_{i=1}^N \check{p}_i \right) \right)}}_{T_2}$$

In order to derive an upper bound for P_{PP} , we examine the trace of the second term, T_2 , in the last expression. This is given by:

$$\begin{aligned} \text{trace}(T_2) &= \frac{2b_2}{N} \text{trace} \left(\frac{\frac{1}{N} \left(\sum_{i=1}^N \check{p}_i \right) \left(\sum_{i=1}^N \check{p}_i^T \right)}{\sum_{i=1}^N (\check{p}_i^T \check{p}_i) - \frac{1}{N} \left(\sum_{i=1}^N \check{p}_i^T \right) \left(\sum_{i=1}^N \check{p}_i \right)} \right) \\ &= \frac{2b_2}{N} \left(\frac{\frac{1}{N} \left(\sum_{i=1}^N \check{p}_i^T \right) \left(\sum_{i=1}^N \check{p}_i \right)}{\sum_{i=1}^N (\check{p}_i^T \check{p}_i) - \frac{1}{N} \left(\sum_{i=1}^N \check{p}_i^T \right) \left(\sum_{i=1}^N \check{p}_i \right)} \right) \\ &= \frac{2b_2}{N} \left(\frac{\frac{1}{N} \left(\sum_{i=1}^N {}^R p_i^T \right) \left(\sum_{i=1}^N {}^R p_i \right)}{\sum_{i=1}^N ({}^R p_i^T {}^R p_i) - \frac{1}{N} \left(\sum_{i=1}^N {}^R p_i^T \right) \left(\sum_{i=1}^N {}^R p_i \right)} \right) \\ &= \frac{2b_2}{N} \left(\frac{\sum_{i=1}^N ({}^R p_i^T {}^R p_i)}{\sum_{i=1}^N ({}^R p_i^T {}^R p_i) - \frac{1}{N} \left(\sum_{i=1}^N {}^R p_i^T \right) \left(\sum_{i=1}^N {}^R p_i \right)} - 1 \right) \\ &= \frac{4b_2}{N} \frac{\sum_{i=1}^N ({}^R p_i^T {}^R p_i)}{\sum_{i=1}^N \sum_{j=1}^N \rho_{ij}^2} - \frac{2b_2}{N} \end{aligned} \quad (66)$$

Thus

$$P_{PP} \preceq \frac{2b_2 + 2Nb_1}{N} I_2 + \text{trace}(T_2) I_2 \quad (67)$$

$$= 2b_1 I_2 + \frac{1}{N} P_{\phi\phi} \sum_{i=1}^N \rho_i^2 I_2 \quad (68)$$

Finally, we observe that the maximum distance between the robot and any landmark is equal to ρ_o , and thus the covariance of the robot's position estimate is bounded above by

$$P_{PP} \preceq (2b_1 + \rho_o^2 P_{\phi\phi}) I_2 \quad (69)$$

This result, along with those of Eqs. (64)-(65), that determine upper bounds on the robot's orientation uncertainty, and that of Eq. (44), which yields the upper bound of the covariance matrix of the global landmark coordinates, are the most important results of this report. They enable us to compute the *guaranteed accuracy* of the state estimates in SLAM, as an *analytical function* of the accuracy of the robot's sensors, and the properties of the landmarks' configuration. Hence, these expressions can be employed in order to determine whether a candidate robot system design satisfies the accuracy requirements of a given SLAM application, *without* the need for simulations, or experimentation.

For example, consider a scenario in which a service robot (e.g., autonomous lawn-mower, autonomous vacuum-cleaner) is operating in an area of approximately known size, and localizes by performing SLAM. Clearly, the state vector should contain as few landmarks as possible, in order to minimize the computational requirements of the localization algorithm. Moreover, the robot's sensors should be as inexpensive (and thus, as inaccurate) as possible, in order to minimize production costs. By employing the results of this work during the design phase, the trade-offs between cost, complexity, and localization accuracy can be studied, and informed decisions can be reached. Moreover, during the robot's operation, the selection of landmarks to include in the state vector can be guided by the results of Eqs. (64)-(65), to ensure *theoretical guarantees* for the robot's pose accuracy. It thus becomes clear that the availability of closed-form expressions that characterize the accuracy of the state estimates in SLAM is a powerful tool, that can be employed in the design of robotic systems. In Section 6, we present results from real-world experiments, that demonstrate the validity of the preceding theoretical analysis.

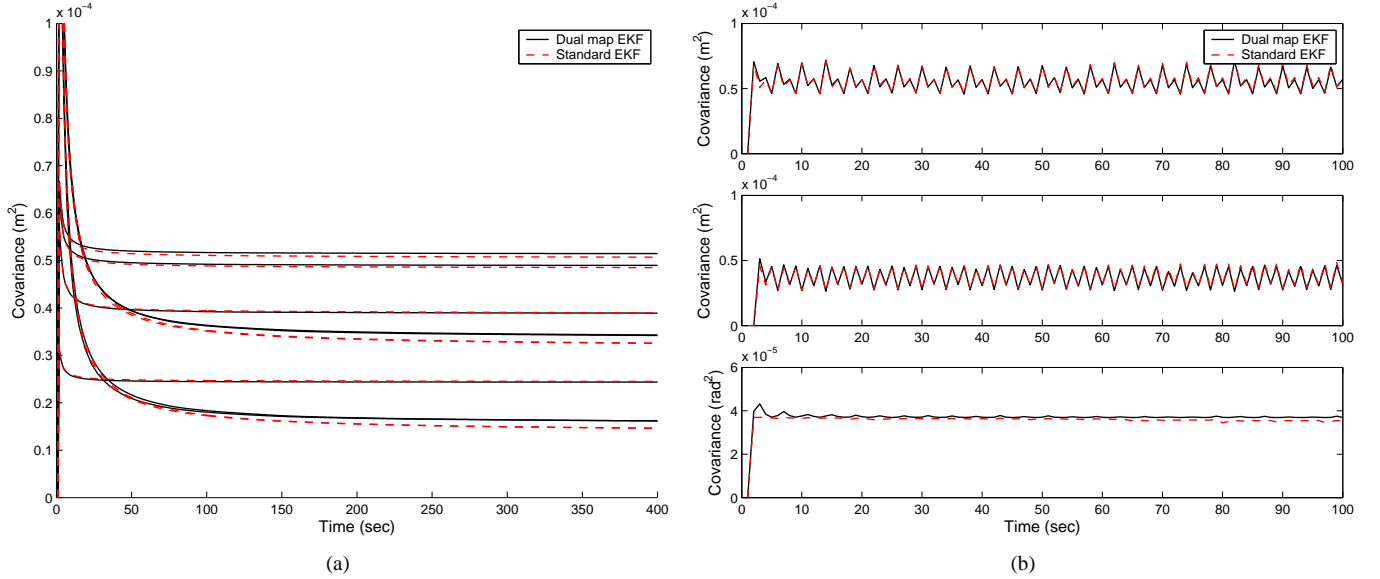


Figure 1: (a) The diagonal elements of the covariance of the landmark position estimates, computed by the standard EKF SLAM algorithm, and by the dual-map filter presented in Section 3. (b) The diagonal elements of the robot pose covariance, computed by the standard EKF SLAM algorithm, and by the method described in Section 5. In order to preserve the clarity of the figure, only the first 100sec are shown.

6 Experimental results

Before describing the setup of our real-world experiments, we illustrate, with numerical results, the equivalence of the SLAM formulation employed in our analysis, to the “standard” EKF SLAM formulation, in which the state vector comprises the robot’s pose and the landmarks’ position estimates in a global frame. For this purpose, we consider a SLAM scenario in which a robot moves randomly in a square area of side 4m, and observes four landmarks randomly placed in the area. Both the “standard” EKF-based SLAM algorithm, and the one described in Section 3, were run with the same data, and the results for the covariance of the global landmark coordinates are shown in Fig. 1(a). In this plot we observe that the numerical results obtained with both filters are almost identical, with the small difference being due to different linearization in the two filters and numerical errors. Moreover, in Fig. 1(b) we plot the diagonal elements of the robot’s pose covariance matrix, computed both by the standard EKF SLAM, and using Eq. (55). Once again, we observe that the two methods yield almost identical results, thus indicating that by studying the properties of the covariance in our formulation, we can draw conclusions for the covariance in the standard EKF-based SLAM algorithm.³

In our real-world experiments, a Pioneer 3 robot equipped with two opposite-facing SICK LMS200 laser scanners, that provide a 360° field of view, was employed (cf. Fig. 2). During the experiment presented in this paper, the robot moves randomly while performing SLAM in an area of approximate dimensions $10\text{m} \times 4\text{m}$. The laser scans are processed for detecting four prominent corners in the area, which are used as landmarks. For detecting each corner, line-fitting is employed to compute the equations of the adjacent wall lines, and the intersection of these lines is determined. The maximum standard deviation of each of the robot-to-landmark measurements was experimentally found to be equal to approximately 0.15m, which yields an upper bound $R \preceq 0.0225I_2\text{m}^2$. The robot receives translational velocity measurements with standard deviation $\sigma_v = 0.01\text{m/sec}$, and rotational velocity measurements with $\sigma_\omega = 5 \times 10^{-3}\text{rad/sec}$. The estimated trajectory of the robot, as well as the landmarks being detected by the robot, are shown in Fig. 3. In the same figure, a sample laser scan is superimposed (after being transformed to the global frame), in order to illustrate the geometry of the area where the robot operates.

In Fig. 4, the standard deviation of the estimation errors, as this is computed by the filter is plotted (solid lines), and compared with the standard deviation computed by employing the theoretically derived bounds (dashed lines). For the robot orientation, the bound in Eq. (65) is employed in this case. Although for this experiment ground truth is not

³We should note that the estimates for the robot’s pose and for the landmarks’ positions computed by the two methods are also practically identical, and the dual-map filter is consistent. The corresponding plots are not included, due to limited space.



Figure 2: The Pioneer 3 robot used in the real-world experiments.

known, we expect that the estimation errors are smaller (in absolute value) than 3 standard deviations, in 99.7% of the cases. From the plots in Fig. 4, we conclude that the analytical bounds that we have derived can be employed in order to *predict* the localization accuracy of SLAM without having to resort to extensive simulations, or experimentation.

We should point out that in this particular case, where the robot moves randomly in space, the actual standard deviations are approximately 2-3 times smaller than the corresponding upper bounds. If the robot’s trajectory was such that the robot-to-landmark distances were always close to their maximum values, the bounds would have been significantly tighter. This fact has been verified in numerous simulation studies of “adverse” SLAM setups. Finally, it is worth mentioning that due to occlusions and data association failures, the landmarks were not detected in every laser scan. On the average, the landmarks were successfully detected 94% of the time. Despite these fluctuations in the number of observed landmarks, the theoretical bounds still provide a quite accurate characterization of the uncertainty in SLAM.

7 Conclusions

In this paper, we have derived upper bounds on the covariance of the state estimates in SLAM, as *analytical* functions of the accuracy of the robot’s sensors, and of the properties of the map (e.g., number of landmarks, maximum distance to landmarks). These bounds determine the *guaranteed accuracy* that will be attained by a robot with a given set of sensors, performing SLAM. Therefore, they can be used during the design of a localization system, to guide the selection of important parameters that affect the system’s performance, cost, and algorithmic complexity. The derived analytical expressions simplify the process of verifying whether a particular design meets the accuracy requirements of a given application, minimizing the need for tedious and time-consuming simulation studies, or exhaustive experimentation. In our future work, we plan to extend these results to cases in which the robot does not operate within the same area for its entire mission. In such cases, the number of visible landmarks dynamically changes over time, and important issues such as loop-closure arise. In this case, the length of the loops of the environment are a crucial factor, that determines the accuracy of the robot’s localization. We believe that the theoretical analysis presented in this paper can serve as a basis for the study of more complex SLAM scenarios.

Acknowledgements

This work was supported by the University of Minnesota (DTC), the NASA Mars Technology Program (MTP-1263201), and the National Science Foundation (EIA-0324864, IIS-0643680).

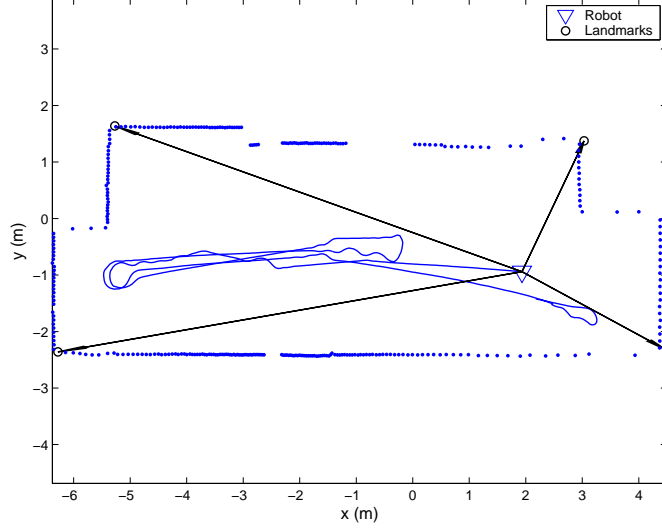


Figure 3: The estimated robot trajectory, as well as the estimated landmark positions, superimposed on a sample laser scan from the area where the robot moves. The arrows indicate the robot-to-landmark measurements.

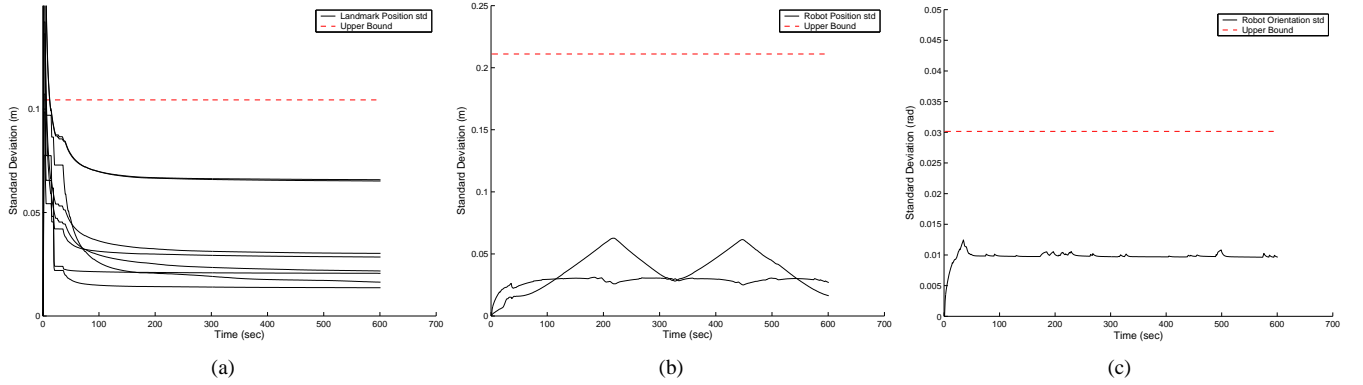


Figure 4: (a) The landmarks' position standard deviation and corresponding upper bound (b) The robot's position standard deviation and corresponding upper bound (c) The robot's orientation standard deviation and corresponding upper bound

A Upper Bound Riccati Recursion

In this appendix we prove that if $\mathbf{R}_u \succeq \mathbf{R}_k$ and $\mathbf{Q}_u \succeq {}^R\mathbf{Q}_k$ for all $k \geq 0$, then the solutions to the following two Riccati recursions

$$\mathbf{P}_{k+1} = \mathbf{P}_k - \mathbf{P}_k \mathbf{H}^T (\mathbf{H} \mathbf{P}_k \mathbf{H}^T + \mathbf{R}_k)^{-1} \mathbf{H} \mathbf{P}_k + \mathbf{G}^R \mathbf{Q}_k \mathbf{G}^T \quad (70)$$

and

$$\mathbf{P}_{k+1}^u = \mathbf{P}_k^u - \mathbf{P}_k^u \mathbf{H}^T (\mathbf{H} \mathbf{P}_k^u \mathbf{H}^T + \mathbf{R}_u)^{-1} \mathbf{H} \mathbf{P}_k^u + \mathbf{G} \mathbf{Q}_u \mathbf{G}^T \quad (71)$$

with the *same* initial condition, \mathbf{P}_0 , satisfy $\mathbf{P}_k^u \succeq \mathbf{P}_k$ for all $k \geq 0$. The proof is carried out by induction, and requires the following two intermediate results:

- **Monotonicity with respect to the measurement covariance matrix**

If $\mathbf{R}_1 \succeq \mathbf{R}_2$, then for any $\mathbf{P} \succeq 0$

$$\mathbf{P} - \mathbf{P} \mathbf{H}^T (\mathbf{H} \mathbf{P} \mathbf{H}^T + \mathbf{R}_1)^{-1} \mathbf{H} \mathbf{P} + \mathbf{Q} \succeq \mathbf{P} - \mathbf{P} \mathbf{H}^T (\mathbf{H} \mathbf{P} \mathbf{H}^T + \mathbf{R}_2)^{-1} \mathbf{H} \mathbf{P} + \mathbf{Q} \quad (72)$$

This statement is proven by taking into account the properties of linear matrix inequalities:

$$\begin{aligned}
\mathbf{R}_1 &\succeq \mathbf{R}_2 \Rightarrow \\
(\mathbf{H}\mathbf{P}\mathbf{H}^T + \mathbf{R}_1)^{-1} &\preceq (\mathbf{H}\mathbf{P}\mathbf{H}^T + \mathbf{R}_2)^{-1} \Rightarrow \\
\mathbf{P}\mathbf{H}^T (\mathbf{H}\mathbf{P}\mathbf{H}^T + \mathbf{R}_1)^{-1} \mathbf{H}\mathbf{P} &\preceq \mathbf{P}\mathbf{H}^T (\mathbf{H}\mathbf{P}\mathbf{H}^T + \mathbf{R}_2)^{-1} \mathbf{H}\mathbf{P} \Rightarrow \\
\Phi \left(\mathbf{P} - \mathbf{P}\mathbf{H}^T (\mathbf{H}\mathbf{P}\mathbf{H}^T + \mathbf{R}_1)^{-1} \mathbf{H}\mathbf{P} \right) \Phi^T &\succeq \Phi \left(\mathbf{P} - \mathbf{P}\mathbf{H}^T (\mathbf{H}\mathbf{P}\mathbf{H}^T + \mathbf{R}_2)^{-1} \mathbf{H}\mathbf{P} \right) \Phi^T \\
\Phi \left(\mathbf{P} - \mathbf{P}\mathbf{H}^T (\mathbf{H}\mathbf{P}\mathbf{H}^T + \mathbf{R}_1)^{-1} \mathbf{H}\mathbf{P} \right) \Phi^T + \mathbf{Q} &\succeq \Phi \left(\mathbf{P} - \mathbf{P}\mathbf{H}^T (\mathbf{H}\mathbf{P}\mathbf{H}^T + \mathbf{R}_2)^{-1} \mathbf{H}\mathbf{P} \right) \Phi^T + \mathbf{Q}
\end{aligned}$$

• **Monotonicity with respect to the state covariance matrix**

The solution to the Riccati recursion at time $k + 1$ is monotonic with to the solution at time k , i.e., if $\mathbf{P}_k^{(1)}$ and $\mathbf{P}_k^{(2)}$ are two different solutions to the same Riccati recursion at time k , with $\mathbf{P}_k^{(1)} \succeq \mathbf{P}_k^{(2)}$ then $\mathbf{P}_{k+1}^{(1)} \succeq \mathbf{P}_{k+1}^{(2)}$. In order to prove the result in the general case, in which $\mathbf{P}_k^{(1)}$ and $\mathbf{P}_k^{(2)}$ are positive semidefinite, we use the following expression that relates the one-step ahead solutions to two Riccati recursions with identical \mathbf{H} , \mathbf{Q} and \mathbf{R} matrices, but different initial values $\mathbf{P}_k^{(1)}$ and $\mathbf{P}_k^{(2)}$ ([20]). It is

$$\mathbf{P}_{k+1}^{(2)} - \mathbf{P}_{k+1}^{(1)} = F_{p,k} \left(\left(\mathbf{P}_k^{(2)} - \mathbf{P}_k^{(1)} \right) - \left(\mathbf{P}_k^{(2)} - \mathbf{P}_k^{(1)} \right) \mathbf{H}^T \left(\mathbf{H}\mathbf{P}_k^{(2)}\mathbf{H}^T + \mathbf{R} \right) \mathbf{H} \left(\mathbf{P}_k^{(2)} - \mathbf{P}_k^{(1)} \right) \right) F_{p,k}^T \quad (73)$$

where $F_{p,k}$ is a matrix whose exact structure is not important for the purposes of this proof. Since we have assumed $\mathbf{P}_k^{(1)} \succeq \mathbf{P}_k^{(2)}$ we can write $\mathbf{P}_k^{(2)} - \mathbf{P}_k^{(1)} \preceq 0$. Additionally, the matrix

$$\left(\mathbf{P}_k^{(2)} - \mathbf{P}_k^{(1)} \right) \mathbf{H}^T \left(\mathbf{H}\mathbf{P}_k^{(2)}\mathbf{H}^T + \mathbf{R} \right) \mathbf{H} \left(\mathbf{P}_k^{(2)} - \mathbf{P}_k^{(1)} \right)$$

is positive semidefinite, and therefore we have

$$\begin{aligned}
- \left(\mathbf{P}_k^{(2)} - \mathbf{P}_k^{(1)} \right) \mathbf{H}^T \left(\mathbf{H}\mathbf{P}_k^{(2)}\mathbf{H}^T + \mathbf{R} \right) \mathbf{H} \left(\mathbf{P}_k^{(2)} - \mathbf{P}_k^{(1)} \right) &\preceq 0 \Rightarrow \\
\left(\mathbf{P}_k^{(2)} - \mathbf{P}_k^{(1)} \right) - \left(\mathbf{P}_k^{(2)} - \mathbf{P}_k^{(1)} \right) \mathbf{H}^T \left(\mathbf{H}\mathbf{P}_k^{(2)}\mathbf{H}^T + \mathbf{R} \right) \mathbf{H} \left(\mathbf{P}_k^{(2)} - \mathbf{P}_k^{(1)} \right) &\preceq 0 \Rightarrow \\
F_{p,k} \left(\left(\mathbf{P}_k^{(2)} - \mathbf{P}_k^{(1)} \right) - \left(\mathbf{P}_k^{(2)} - \mathbf{P}_k^{(1)} \right) \mathbf{H}^T \left(\mathbf{H}\mathbf{P}_k^{(2)}\mathbf{H}^T + \mathbf{R} \right) \mathbf{H} \left(\mathbf{P}_k^{(2)} - \mathbf{P}_k^{(1)} \right) \right) F_{p,k}^T &\preceq 0 \Rightarrow \\
\mathbf{P}_{k+1}^{(2)} - \mathbf{P}_{k+1}^{(1)} &\preceq 0
\end{aligned}$$

The last line implies that $\mathbf{P}_{k+1}^{(1)} \succeq \mathbf{P}_{k+1}^{(2)}$, which is the desired result.

We can now employ induction to prove the main statement of this appendix. Assuming that at some time instant i , $\mathbf{P}_i^u \succeq \mathbf{P}_i$, we can write

$$\begin{aligned}
\mathbf{P}_{i+1}^u &= \Phi_i \left(\mathbf{P}_i^u - \mathbf{P}_i^u \mathbf{H}^T \left(\mathbf{H}\mathbf{P}_i^u\mathbf{H}^T + \mathbf{R}_u \right)^{-1} \mathbf{H}\mathbf{P}_i^u \right) \Phi_i^T + \mathbf{G}\mathbf{Q}_{u_i}\mathbf{G}^T \\
&\succeq \Phi_i \left(\mathbf{P}_i - \mathbf{P}_i \mathbf{H}^T \left(\mathbf{H}\mathbf{P}_i\mathbf{H}^T + \mathbf{R}_u \right)^{-1} \mathbf{H}\mathbf{P}_i \right) \Phi_i^T + \mathbf{G}\mathbf{Q}_{u_i}\mathbf{G}^T \\
&\succeq \Phi_i \left(\mathbf{P}_i - \mathbf{P}_i \mathbf{H}^T \left(\mathbf{H}\mathbf{P}_i\mathbf{H}^T + \mathbf{R}_u \right)^{-1} \mathbf{H}\mathbf{P}_i \right) \Phi_i^T + \mathbf{G}^R \mathbf{Q}_i \mathbf{G}^T \\
&\succeq \Phi_i \left(\mathbf{P}_i - \mathbf{P}_i \mathbf{H}^T \left(\mathbf{H}\mathbf{P}_i\mathbf{H}^T + \mathbf{R}(k+1) \right)^{-1} \mathbf{H}\mathbf{P}_i \right) \Phi_i^T + \mathbf{G}^R \mathbf{Q}_i \mathbf{G}^T = \mathbf{P}_{i+1}
\end{aligned}$$

where the monotonicity of the Riccati recursion with respect to the covariance matrix, the property $\mathbf{Q}_{u_i} \succeq {}^R\mathbf{Q}_i$ and the monotonicity of the Riccati recursion with respect to the measurement covariance matrix have been used in the last three lines. Thus $\mathbf{P}_i^u \succeq \mathbf{P}_i \Rightarrow \mathbf{P}_{i+1}^u \succeq \mathbf{P}_{i+1}$. For $i = 0$ the condition $\mathbf{P}_i^u \succeq \mathbf{P}_i$ holds, and therefore the proof by induction is complete.

B Proof of Lemma 4.2

First, we note that the properties in Eq. (37) are equivalent to the expression:

$$\mathbf{P}_k^u = \mathbf{C}_k \bar{\mathbf{P}}_k \mathbf{C}_k^T \quad (74)$$

where

$$\mathbf{C}_k = \Phi_k \cdot \Phi_{k-1} \cdots \Phi_0$$

We will prove the above property by induction. Let's assume that this property holds for $k = \ell$, i.e., that:

$$\mathbf{P}_\ell^u = \mathbf{C}_\ell \bar{\mathbf{P}}_\ell \mathbf{C}_\ell^T \quad (75)$$

From the Riccati recursion we obtain:

$$\begin{aligned} \mathbf{P}_{\ell+1}^u &= \Phi_{\ell+1} \left(\mathbf{P}_\ell^u - \mathbf{P}_\ell^u \mathbf{H}^T (\mathbf{H} \mathbf{P}_\ell^u \mathbf{H}^T + \mathbf{R}_u)^{-1} \mathbf{H} \mathbf{P}_\ell^u \right) \Phi_{\ell+1}^T + \mathbf{G} \mathbf{Q}_u \mathbf{G}^T \\ &= \Phi_{\ell+1} \left(\mathbf{P}_\ell^u - \mathbf{P}_\ell^u \mathbf{H}^T (\mathbf{H} \mathbf{P}_\ell^u \mathbf{H}^T + \mathbf{R}_u)^{-1} \mathbf{H} \mathbf{P}_\ell^u + \mathbf{G} \mathbf{Q}_u \mathbf{G}^T \right) \Phi_{\ell+1}^T \end{aligned} \quad (76)$$

In the last expression, we have employed the property (cf. Eqs. (7), (10), and (32)):

$$\mathbf{G} \mathbf{Q}_u \mathbf{G}^T = \begin{bmatrix} q_1(\mathbf{1}_{N \times N} \otimes I_2) + q_2 I_{2N} & \mathbf{0}_{2N \times 2N} \\ \mathbf{0}_{2N \times 2N} & \mathbf{0}_{2N \times 2N} \end{bmatrix} \quad (77)$$

$$= \Phi_{\ell+1} \begin{bmatrix} q_1(\mathbf{1}_{N \times N} \otimes I_2) + q_2 I_{2N} & \mathbf{0}_{2N \times 2N} \\ \mathbf{0}_{2N \times 2N} & \mathbf{0}_{2N \times 2N} \end{bmatrix} \Phi_{\ell+1}^T \quad (78)$$

$$= \Phi_{\ell+1} \mathbf{G} \mathbf{Q}_u \mathbf{G}^T \Phi_{\ell+1}^T \quad (79)$$

Substitution from Eq. (75) into (76), yields:

$$\begin{aligned} \mathbf{P}_{\ell+1}^u &= \Phi_{\ell+1} \left(\mathbf{C}_\ell \bar{\mathbf{P}}_\ell \mathbf{C}_\ell^T - \mathbf{C}_\ell \bar{\mathbf{P}}_\ell \mathbf{C}_\ell^T \mathbf{H}^T (\mathbf{H} \mathbf{C}_\ell \bar{\mathbf{P}}_\ell \mathbf{C}_\ell^T \mathbf{H}^T + \mathbf{R}_u)^{-1} \mathbf{H} \mathbf{C}_\ell \bar{\mathbf{P}}_\ell \mathbf{C}_\ell^T + \mathbf{G} \mathbf{Q}_u \mathbf{G}^T \right) \Phi_{\ell+1}^T \\ &= \Phi_{\ell+1} \mathbf{C}_\ell \left(\bar{\mathbf{P}}_\ell - \bar{\mathbf{P}}_\ell \mathbf{C}_\ell^T \mathbf{H}^T (\mathbf{H} \mathbf{C}_\ell \bar{\mathbf{P}}_\ell \mathbf{C}_\ell^T \mathbf{H}^T + \mathbf{R}_u)^{-1} \mathbf{H} \mathbf{C}_\ell \bar{\mathbf{P}}_\ell + \mathbf{G} \mathbf{Q}_u \mathbf{G}^T \right) \mathbf{C}_\ell^T \Phi_{\ell+1}^T \\ &= \mathbf{C}_{\ell+1} \left(\bar{\mathbf{P}}_\ell - \bar{\mathbf{P}}_\ell \mathbf{C}_\ell^T \mathbf{H}^T (\mathbf{H} \mathbf{C}_\ell \bar{\mathbf{P}}_\ell \mathbf{C}_\ell^T \mathbf{H}^T + \mathbf{R}_u)^{-1} \mathbf{H} \mathbf{C}_\ell \bar{\mathbf{P}}_\ell + \mathbf{G} \mathbf{Q}_u \mathbf{G}^T \right) \mathbf{C}_{\ell+1}^T \end{aligned} \quad (80)$$

At this point, we employ the following relations, which can be easily verified:

$$\mathbf{C}_\ell^T \mathbf{H}^T = \mathbf{H}^T \mathbf{C}_\ell^T \quad (81)$$

$$\mathbf{R}_u = \mathbf{C}_\ell \mathbf{R}_u \mathbf{C}_\ell^T \quad (82)$$

Substitution in Eq. (80) yields

$$\begin{aligned} \mathbf{P}_{\ell+1}^u &= \mathbf{C}_{\ell+1} \left(\bar{\mathbf{P}}_\ell - \bar{\mathbf{P}}_\ell \mathbf{H}^T \mathbf{R}_u^{-1} \mathbf{H} \mathbf{C}_\ell^T \left(\mathbf{C}_\ell \bar{\mathbf{P}}_\ell \mathbf{C}_\ell^T \mathbf{H}^T \mathbf{R}_u^{-1} \mathbf{H} \mathbf{C}_\ell \bar{\mathbf{P}}_\ell + \mathbf{G} \mathbf{Q}_u \mathbf{G}^T \right)^{-1} \mathbf{R}_u \mathbf{C}_\ell \bar{\mathbf{P}}_\ell + \mathbf{G} \mathbf{Q}_u \mathbf{G}^T \right) \mathbf{C}_{\ell+1}^T \\ &= \mathbf{C}_{\ell+1} \left(\bar{\mathbf{P}}_\ell - \bar{\mathbf{P}}_\ell \mathbf{H}^T (\mathbf{H} \bar{\mathbf{P}}_\ell \mathbf{H}^T + \mathbf{R}_u)^{-1} \mathbf{H} \bar{\mathbf{P}}_\ell + \mathbf{G} \mathbf{Q}_u \mathbf{G}^T \right) \mathbf{C}_{\ell+1}^T \\ &= \mathbf{C}_{\ell+1} \bar{\mathbf{P}}_{\ell+1} \mathbf{C}_{\ell+1}^T \end{aligned} \quad (83)$$

We have thus shown that if the property of Eq. (75) holds for time index ℓ , it then also holds for time index $\ell + 1$. For $\ell = 0$, the property can be easily shown to hold, since $\mathbf{C}_0 = I_{2N}$. Thus, the proof by induction is complete.

C Steady-state solution of the Riccati recursion

In this appendix we derive the steady-state solution to the Riccati recursion in Eq. (35), by employing Lemma 4.3. The derivations comprise three intermediate results:

C.1 Intermediate Result 1

We first derive the solution to Eq. (35) with zero initial condition. As explained, in this case the submatrix of $\bar{\mathbf{P}}_k$ corresponding to the global map is equal to zero for all k . Therefore, the only submatrix of $\bar{\mathbf{P}}_k$ with nonzero value is the submatrix ${}^R\bar{\mathbf{P}}_k$, which corresponds to the relative map. To simplify the derivations, we introduce the eigenvalue decomposition of the matrix \mathbf{Q}_u , which we denote as

$$\mathbf{Q}_u = \mathbf{U}\mathbf{\Lambda}\mathbf{U}^T = \mathbf{U} \text{diag}(\lambda_i)\mathbf{U}^T$$

Substitution of the values of the matrices \mathbf{H} , \mathbf{G} , \mathbf{R}_u and \mathbf{Q}_u in Eq. (35), leads to the following recursion for ${}^R\bar{\mathbf{P}}_k$:

$${}^R\bar{\mathbf{P}}_{k+1} = {}^R\bar{\mathbf{P}}_k - {}^R\bar{\mathbf{P}}_k ({}^R\bar{\mathbf{P}}_k + rI_{2N})^{-1} {}^R\bar{\mathbf{P}}_k + \mathbf{U}\mathbf{\Lambda}\mathbf{U}^T \Rightarrow \quad (84)$$

$$\mathbf{U}^T {}^R\bar{\mathbf{P}}_k \mathbf{U} = \mathbf{U}^T {}^R\bar{\mathbf{P}}_k \mathbf{U} - \mathbf{U}^T {}^R\bar{\mathbf{P}}_k \mathbf{U} (\mathbf{U}^T {}^R\bar{\mathbf{P}}_k \mathbf{U} + rI_{2N})^{-1} \mathbf{U}^T {}^R\bar{\mathbf{P}}_k \mathbf{U} + \mathbf{\Lambda} \Rightarrow \quad (85)$$

$$\bar{\mathbf{P}}_{n_{k+1}} = \bar{\mathbf{P}}_{n_k} - \bar{\mathbf{P}}_{n_k} \mathbf{U} (\bar{\mathbf{P}}_{n_k} + rI_{2N})^{-1} \bar{\mathbf{P}}_{n_k} + \mathbf{\Lambda} \quad (86)$$

where we have denoted

$$\bar{\mathbf{P}}_{n_k} = \mathbf{U}^T {}^R\bar{\mathbf{P}}_k \mathbf{U} \quad (87)$$

We note that since $\bar{\mathbf{P}}_{n_k}$ is initially zero, and the matrix coefficients in the above recursion are diagonal, $\bar{\mathbf{P}}_{n_k}$ will retain a diagonal structure for all time. The steady-state value of $\bar{\mathbf{P}}_{n_k}$, which we denote as $\bar{\mathbf{P}}_{n_\infty} = \text{diag}(p_{\infty_i})$, is found by solving the equations:

$$p_{\infty_i} = p_{\infty_i} - \frac{p_{\infty_i}^2}{p_{\infty_i} + r} + \lambda_i, i = 1, \dots, 2N \quad (88)$$

Solving these equations and substituting in Eq. (87), we obtain the following steady-state solution for ${}^R\bar{\mathbf{P}}_k$:

$${}^R\bar{\mathbf{P}}_\infty = \mathbf{U} \text{diag} \left(\frac{\lambda_i}{2} + \sqrt{\frac{\lambda_i^2}{4} + \lambda_i r} \right) \mathbf{U}^T \quad (89)$$

and therefore the steady state solution to the Riccati in Eq. (35) with zero initial condition is given by

$$\bar{\mathbf{P}}_\infty^{(0)} = \begin{bmatrix} \mathbf{U} \text{diag} \left(\frac{\lambda_i}{2} + \sqrt{\frac{\lambda_i^2}{4} + \lambda_i r} \right) \mathbf{U}^T & \mathbf{0}_{2N \times 2N} \\ \mathbf{0}_{2N \times 2N} & \mathbf{0}_{2N \times 2N} \end{bmatrix} \quad (90)$$

C.2 Intermediate Result 2

We next derive the steady-state solution to the dual Riccati in Eq. (41). Substituting the values of the matrices \mathbf{H} , \mathbf{G} , \mathbf{R}_u and \mathbf{Q}_u in this recursion, and studying the block structure of the matrices that appear in it, leads to the observation that all block submatrices of \mathbf{J}_k , except for the one corresponding to the relative map, remain zero. The time evolution of this submatrix is described by the recursion:

$${}^R\mathbf{J}_{k+1} = {}^R\mathbf{J}_k + \frac{1}{r}I_{2N} - {}^R\mathbf{J}_k \left({}^R\mathbf{J}_k + \mathbf{U} \text{diag} \left(\frac{1}{\lambda_i} \right) \mathbf{U} \right)^{-1} {}^R\mathbf{J}_k \Rightarrow \quad (91)$$

$$\mathbf{U}^T {}^R\mathbf{J}_{k+1} \mathbf{U} = \mathbf{U}^T {}^R\mathbf{J}_k \mathbf{U} + \frac{1}{r}I_{2N} - \mathbf{U}^T {}^R\mathbf{J}_k \mathbf{U} \left(\mathbf{U}^T {}^R\mathbf{J}_k \mathbf{U} + \text{diag} \left(\frac{1}{\lambda_i} \right) \right)^{-1} \mathbf{U}^T {}^R\mathbf{J}_k \mathbf{U} \Rightarrow \quad (92)$$

$$\mathbf{J}_{n_{k+1}} = \mathbf{J}_{n_k} + \frac{1}{r}I_{2N} - \mathbf{J}_{n_k} \left(\mathbf{J}_{n_k} + \text{diag} \left(\frac{1}{\lambda_i} \right) \right)^{-1} \mathbf{J}_{n_k} \quad (93)$$

where we have defined

$$\mathbf{J}_{n_k} = \mathbf{U}^T {}^R\mathbf{J}_k \mathbf{U} \quad (94)$$

Similarly to the case of $\bar{\mathbf{P}}_{n_k}$, we observe that \mathbf{J}_{n_k} remains diagonal for all time. Its asymptotic value is found by setting $\mathbf{J}_{n_k} = \mathbf{J}_{n_{k+1}} = \mathbf{J}_{n_\infty}$, and is equal to

$$\mathbf{J}_{n_\infty} = \text{diag} \left(\frac{1}{2r} + \sqrt{\frac{1}{4r^2} + \frac{1}{\lambda_i r}} \right)$$

Therefore, the steady-state value of ${}^R\mathbf{J}_k$ is

$${}^R\mathbf{J}_\infty = \mathbf{U} \text{diag} \left(\frac{1}{2r} + \sqrt{\frac{1}{4r^2} + \frac{1}{\lambda_i r}} \right) \mathbf{U}^T = \mathbf{U} \text{diag}(\mathbf{J}_{n_\infty}) \mathbf{U}^T \quad (95)$$

and the asymptotic solution of the dual Riccati with zero initial condition is given by

$$\mathbf{J}_\infty = \begin{bmatrix} {}^R\mathbf{J}_\infty & \mathbf{0}_{2N \times 2N} \\ \mathbf{0}_{2N \times 2N} & \mathbf{0}_{2N \times 2N} \end{bmatrix} = \begin{bmatrix} \mathbf{U} \text{diag} \left(\frac{1}{2r} + \sqrt{\frac{1}{4r^2} + \frac{1}{\lambda_i r}} \right) \mathbf{U}^T & \mathbf{0}_{2N \times 2N} \\ \mathbf{0}_{2N \times 2N} & \mathbf{0}_{2N \times 2N} \end{bmatrix} \quad (96)$$

C.3 Intermediate Result 3

The solution requires computation of the asymptotic value of the right-hand side of Eq. (38). For this purpose, we now compute the asymptotic value of the matrix \mathbf{T}_k (cf. Eq. (39)). We first note that $\bar{\mathbf{P}}_\infty^{(0)}$ is a solution to the DARE in Eq. (40) (this can be verified by substitution), and thus

$$\begin{aligned} \mathbf{T}_k &= (I_{4N} - \mathbf{K}_p \mathbf{H})^k (I_{4N} + \mathbf{P} \mathbf{J}_k) \\ &= \left(I_{4N} - \bar{\mathbf{P}}_\infty^{(0)} \mathbf{H}^T \left(\mathbf{R}_u + \mathbf{H} \bar{\mathbf{P}}_\infty^{(0)} \mathbf{H}^T \right)^{-1} \mathbf{H} \right)^k (I_{4N} + \bar{\mathbf{P}}_\infty^{(0)} \mathbf{J}_k) \\ &= \begin{bmatrix} \left(I_{2N} - {}^R\bar{\mathbf{P}}_\infty^{(0)} \left(r I_{2N} + {}^R\bar{\mathbf{P}}_\infty^{(0)} \right)^{-1} \right)^k & \mathbf{0}_{2N \times 2N} \\ \mathbf{0}_{2N \times 2N} & I_{2N} \end{bmatrix} (I_{4N} + \bar{\mathbf{P}}_\infty^{(0)} \mathbf{J}_k) \\ &= \begin{bmatrix} \mathbf{U} \text{diag} \left(1 - \frac{p_\infty}{r + p_\infty} \right)^k \mathbf{U}^T & \mathbf{0}_{2N \times 2N} \\ \mathbf{0}_{2N \times 2N} & I_{2N} \end{bmatrix} (I_{4N} + \bar{\mathbf{P}}_\infty^{(0)} \mathbf{J}_k) \end{aligned}$$

At this point we note that

$$1 - \frac{p_\infty}{r + p_\infty} < 1$$

and thus

$$\lim_{k \rightarrow \infty} \left(1 - \frac{p_\infty}{r + p_\infty} \right)^k = 0$$

Therefore, we obtain

$$\lim_{k \rightarrow \infty} \mathbf{T}_k = \begin{bmatrix} \mathbf{0}_{2N \times 2N} & \mathbf{0}_{2N \times 2N} \\ \mathbf{0}_{2N \times 2N} & I_{2N} \end{bmatrix} \quad (97)$$

C.4 Derivation of Eq. (42)

To compute the steady-state solution to Eq. (35), we evaluate the right-hand side of Eq. (38) as $k \rightarrow \infty$. Substitution from Eqs. (33), (96) and (97) yields:

$$\begin{aligned} \bar{\mathbf{P}}_\infty - \bar{\mathbf{P}}_\infty^{(0)} &= \mathbf{T}_\infty (I_{4N} + \bar{\mathbf{P}}_0 \mathbf{J}_\infty)^{-1} \bar{\mathbf{P}}_0 \mathbf{T}_\infty^T \\ &= \begin{bmatrix} \mathbf{0}_{2N \times 2N} & \mathbf{0}_{2N \times 2N} \\ \mathbf{0}_{2N \times 2N} & I_{2N} \end{bmatrix} \begin{bmatrix} I_{2N} + (\mathbf{Q}_u + r I_{2N}) {}^R\mathbf{J}_\infty & \mathbf{0}_{2N \times 2N} \\ r {}^R\mathbf{J}_\infty I_{2N} & I_{2N} \end{bmatrix}^{-1} \\ &\quad \times \begin{bmatrix} (\mathbf{Q}_u + r I_{2N}) & r I_{2N} \\ r I_{2N} & r I_{2N} \end{bmatrix} \begin{bmatrix} \mathbf{0}_{2N \times 2N} & \mathbf{0}_{2N \times 2N} \\ \mathbf{0}_{2N \times 2N} & I_{2N} \end{bmatrix} \end{aligned} \quad (98)$$

$$\begin{aligned}
&= \begin{bmatrix} \mathbf{0}_{2N \times 2N} & \mathbf{0}_{2N \times 2N} \\ \mathbf{0}_{2N \times 2N} & I_{2N} \end{bmatrix} \begin{bmatrix} \mathbf{U} \text{diag}(1 + (\lambda_i + r)J_{\infty_i}) \mathbf{U}^T & \mathbf{0}_{2N \times 2N} \\ -\mathbf{U} \text{diag}(rJ_{\infty_i}) \mathbf{U}^T & I_{2N} \end{bmatrix}^{-1} \begin{bmatrix} \mathbf{0}_{2N \times 2N} & rI_{2N} \\ \mathbf{0}_{2N \times 2N} & rI_{2N} \end{bmatrix} \\
&= \begin{bmatrix} \mathbf{0}_{2N \times 2N} & \mathbf{0}_{2N \times 2N} \\ \mathbf{0}_{2N \times 2N} & I_{2N} \end{bmatrix} \begin{bmatrix} \mathbf{U} \text{diag}\left(\frac{1}{1 + (\lambda_i + r)J_{\infty_i}}\right) \mathbf{U}^T & \mathbf{0}_{2N \times 2N} \\ -\mathbf{U} \text{diag}\left(\frac{rJ_{\infty_i}}{1 + (\lambda_i + r)J_{\infty_i}}\right) \mathbf{U}^T & I_{2N} \end{bmatrix} \begin{bmatrix} \mathbf{0}_{2N \times 2N} & rI_{2N} \\ \mathbf{0}_{2N \times 2N} & rI_{2N} \end{bmatrix} \\
&= \begin{bmatrix} \mathbf{0}_{2N \times 2N} & \mathbf{0}_{2N \times 2N} \\ \mathbf{0}_{2N \times 2N} & \mathbf{U} \text{diag}\left(r - \frac{r^2 J_{\infty_i}}{1 + (\lambda_i + r)J_{\infty_i}}\right) \mathbf{U}^T \end{bmatrix} \quad (99)
\end{aligned}$$

Substitution for the values of J_{∞_i} from Eq. (95) in the last expression, and simple algebraic manipulation, yields

$$\bar{\mathbf{P}}_{\infty} - \bar{\mathbf{P}}_{\infty}^{(0)} = \begin{bmatrix} \mathbf{0}_{2N \times 2N} & \mathbf{0}_{2N \times 2N} \\ \mathbf{0}_{2N \times 2N} & \mathbf{U} \text{diag}\left(-\frac{\lambda_i}{2} + \sqrt{\frac{\lambda_i^2}{4} + \lambda_i r}\right) \mathbf{U}^T \end{bmatrix} \quad (100)$$

Combining the last result with that of Eq. (90), we obtain

$$\bar{\mathbf{P}}_{\infty} = \begin{bmatrix} \mathbf{U} \text{diag}\left(\frac{\lambda_i}{2} + \sqrt{\frac{\lambda_i^2}{4} + \lambda_i r}\right) \mathbf{U}^T & \mathbf{0}_{2N \times 2N} \\ \mathbf{0}_{2N \times 2N} & \mathbf{U} \text{diag}\left(-\frac{\lambda_i}{2} + \sqrt{\frac{\lambda_i^2}{4} + \lambda_i r}\right) \mathbf{U}^T \end{bmatrix} \quad (101)$$

D Matrix Inversion Lemma

If A is $n \times n$, B is $n \times m$, C is $m \times m$ and D is $m \times n$ then:

$$(A^{-1} + BC^{-1}D)^{-1} = A - AB(DAB + C)^{-1}DA \quad (102)$$

E Inversion of a Partitioned Matrix

Let a $(m + n) \times (m + n)$ matrix K be partitioned as

$$K = \begin{bmatrix} A & B \\ C & D \end{bmatrix}$$

Where the $m \times m$ matrix A and the $n \times n$ matrix D are invertible. Then the inverse matrix of K can be written as

$$\begin{bmatrix} X & Y \\ Z & U \end{bmatrix} = \begin{bmatrix} (A - BD^{-1}C)^{-1} & -A^{-1}B(D - CA^{-1}B)^{-1} \\ -D^{-1}C(A - BD^{-1}C)^{-1} & (D - CA^{-1}B)^{-1} \end{bmatrix} \quad (103)$$

References

- [1] M. Montemerlo, “FastSLAM: A factored solution to the simultaneous localization and mapping problem with unknown data association,” Ph.D. dissertation, Robotics Institute, Carnegie Mellon University, 2003.
- [2] P. Newman, J. Leonard, J. D. Tardos, and J. Neira, “Explore and return: experimental validation of real-time concurrent mapping and localization,” in *Proc. of the IEEE International Conference on Robotics and Automation*, Washington, DC, May 11-15 2002, pp. 1802–9.
- [3] S. B. Williams, G. Dissanayake, and H. Durrant-Whyte, “An efficient approach to the simultaneous localisation and mapping problem,” in *Proc. of the 2002 IEEE International Conference on Robotics and Automation*, Washington, DC, May 11-15 2002, pp. 406–11.
- [4] S. Thrun, Y. Liu, D. Koller, A. Ng, Z. Ghahramani, and H. Durrant-Whyte, “Simultaneous localization and mapping with sparse extended information filters,” *International Journal of Robotics Research*, vol. 23, no. 7-8, pp. 693–716, Aug. 2004.

- [5] M. Paskin, "Thin junction tree filters for simultaneous localization and mapping," Ph.D. dissertation, Berkeley, 2002.
- [6] J. Neira and J. D. Tardos, "Data association in stochastic mapping using the joint compatibility test," *IEEE Transactions on Robotics and Automation*, vol. 17, no. 6, pp. 890–897, 2001.
- [7] S. Se, D. G. Lowe, and J. Little, "Mobile robot localization and mapping with uncertainty using scale-invariant visual landmarks," *International Journal of Robotics Research*, vol. 21, no. 8, pp. 735–758, 2002.
- [8] F. Tang, M. Adams, J. Ibanez-Guzman, and S. Wijesoma, "Pose invariant, robust feature extraction from range data with a modified scale space approach," in *Proc. of the IEEE International Conference on Robotics and Automation*, New Orleans, LA, Apr 26-May 1 2004, pp. 3173–3179.
- [9] A. I. Mourikis and S. I. Roumeliotis, "Analysis of positioning uncertainty in simultaneous localization and mapping (SLAM)," in *Proc. of the IEEE/RSJ International Conference on Robotics and Intelligent Systems (IROS)*, Sendai, Japan, September 28 - October 2 2004, pp. 13–20.
- [10] —, "Performance bounds for cooperative simultaneous localization and mapping (C-SLAM)," in *Proc. of Robotics: Science and Systems Conference*, Cambridge, MA, June 8-11 2005, pp. 73–80.
- [11] P. W. Gibbens, G. M. W. M. Dissanayake, and H. F. Durrant-Whyte, "A Closed Form Solution to the Single Degree of Freedom Simultaneous Localisation and Map Building (SLAM) Problem," in *Proceedings of the 39th IEEE Conference on Decision and Control*, Sydney, NSW, Australia, 12-15 December 2000, pp. 191–196.
- [12] E. W. Nettleton, P. W. Gibbens, and H. F. Durrant-Whyte, "Closed form solutions to the multiple platform simultaneous localization and map building (SLAM) problem," in *Sensor Fusion: Architectures, Algorithms, and Applications IV*, B. V. Dasarathy, Ed., vol. 4051, Bellingham, WA, 2000, pp. 428–437.
- [13] P. M. Newman, "On the Structure and Solution of the Simultaneous Localisation and Map Building Problem," Ph.D. dissertation, University of Sydney, March 1999.
- [14] M. Csorba, "Simultaneous Localization and Map Building," Ph.D. dissertation, University of Oxford, 1997.
- [15] G. M. W. M. Dissanayake, P. M. Newman, H. F. Durrant-Whyte, S. Clark, and M. Csorba, "A Solution to the Simultaneous Localization and Map Building (SLAM) Problem," *IEEE Transactions of Robotics and Automation*, vol. 17, no. 3, pp. 229–241, June 2001.
- [16] J. W. Fenwick, P. M. Newman, and J. J. Leonard, "Cooperative Concurrent Mapping and Localization," in *Proceedings of the 2002 IEEE International Conference on Robotics and Automation*, Washington D.C., 11-15 May 2002, pp. 1810–1817.
- [17] J. W. Fenwick, "Collaborative Concurrent Mapping and Localization," Master's thesis, Massachusetts Institute of Technology, June 2001.
- [18] R. C. Smith, M. Self, and P. Cheeseman, *Autonomous Robot Vehicles*. Springer-Verlag, 1990, ch. Estimating Uncertain Spatial Relationships in Robotics, pp. 167–193.
- [19] J. Leonard, R. Rikoski, P. Newman, and M. Bosse, "Mapping partially observable features from multiple uncertain vantage points," *The International Journal of Robotics Research*, vol. 21, no. 10-11, pp. 943–975, 2002.
- [20] B. Hassibi, "Indefinite metric spaces in estimation, control and adaptive filtering," Ph.D. dissertation, Stanford University, August 1996.